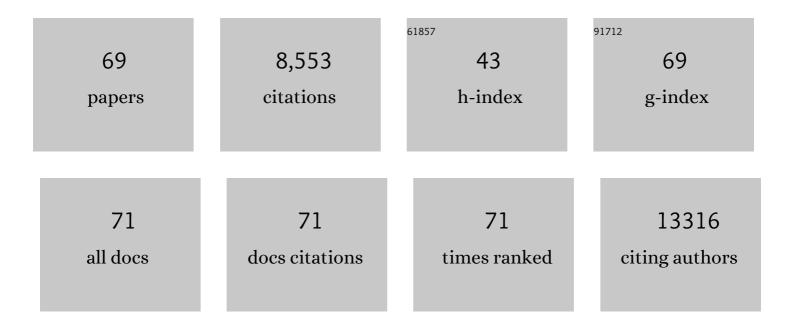
List of Publications by Year in descending order

Source: https://exaly.com/author-pdf/2754551/publications.pdf Version: 2024-02-01



FENC WANC

#	Article	IF	CITATIONS
1	Crystallization Regulation and Morphological Evolution for HTMâ€free Tin‣ead (1.28eV) Alloyed Perovskite Solar Cells. Energy and Environmental Materials, 2023, 6, .	7.3	8
2	Temperatureâ€Insensitive Efficient Inorganic Perovskite Photovoltaics by Bulk Heterojunctions. Advanced Materials, 2022, , 2108357.	11.1	9
3	Rare-Earth Doping in Nanostructured Inorganic Materials. Chemical Reviews, 2022, 122, 5519-5603.	23.0	338
4	Recent advancements and future insight of lead-free non-toxic perovskite solar cells for sustainable and clean energy production: A review. Sustainable Energy Technologies and Assessments, 2022, 53, 102433.	1.7	20
5	Functional Thin Films for Perovskite Solar Cells. Coatings, 2022, 12, 952.	1.2	0
6	The atomic-level structure of bandgap engineered double perovskite alloys Cs <sub>2</sub> AgIn <sub>1â~'<i>x</i></sub> Fe <sub><i>x</i></sub> Cl <sub>6</sub> . Chemical Science, 2021, 12, 1730-1735.	3.7	34
7	Improving the efficiency and stability of tin-based perovskite solar cells using anilinium hypophosphite additive. New Journal of Chemistry, 2021, 45, 8092-8100.	1.4	10
8	Strong self-trapping by deformation potential limits photovoltaic performance in bismuth double perovskite. Science Advances, 2021, 7, .	4.7	98
9	Efficient Stabilization and Passivation for Low-Temperature-Processed Î <sup>3</sup> -CsPbI3 Solar Cells. ACS Applied Materials & Interfaces, 2021, 13, 18784-18791.	4.0	11
10	Optoelectronic property refinement of FASnI3 films for photovoltaic application. Materials Letters, 2021, 300, 130099.	1.3	2
11	Application of two-dimensional materials in perovskite solar cells: recent progress, challenges, and prospective solutions. Journal of Materials Chemistry C, 2021, 9, 14065-14092.	2.7	24
12	Nearâ€Infrared Lightâ€Responsive Cuâ€Doped Cs <sub>2</sub> AgBiBr <sub>6</sub> . Advanced Functional Materials, 2020, 30, 2005521.	7.8	56
13	Leadâ€Free Halide Double Perovskite Cs <sub>2</sub> AgBiBr <sub>6</sub> with Decreased Band Gap. Angewandte Chemie - International Edition, 2020, 59, 15191-15194.	7.2	80
14	Leadâ€Free Halide Double Perovskite Cs <sub>2</sub> AgBiBr <sub>6</sub> with Decreased Band Gap. Angewandte Chemie, 2020, 132, 15303-15306.	1.6	34
15	Efficient perovskite solar cells enabled by ion-modulated grain boundary passivation with a fill factor exceeding 84%. Journal of Materials Chemistry A, 2019, 7, 22359-22365.	5.2	33
16	Thermochromic Leadâ€Free Halide Double Perovskites. Advanced Functional Materials, 2019, 29, 1807375.	7.8	120
17	Fundamentals of Solar Cells and Light-Emitting Diodes. , 2019, , 1-35.		4
18	Pulsed Terahertz Emission from Solution-Processed Lead Iodide Perovskite Films. ACS Photonics, 2019, 6. 1175-1181.	3.2	21

#	Article	IF	CITATIONS
19	Long Electron–Hole Diffusion Length in Highâ€Quality Leadâ€Free Double Perovskite Films. Advanced Materials, 2018, 30, e1706246.	11.1	242
20	Defects engineering for high-performance perovskite solar cells. Npj Flexible Electronics, 2018, 2, .	5.1	334
21	Textured CH3NH3PbI3 thin film with enhanced stability for high performance perovskite solar cells. Nano Energy, 2017, 33, 485-496.	8.2	74
22	Benzylamineâ€Treated Wideâ€Bandgap Perovskite with High Thermalâ€Photostability and Photovoltaic Performance. Advanced Energy Materials, 2017, 7, 1701048.	10.2	188
23	Organic Cationâ€Dependent Degradation Mechanism of Organotin Halide Perovskites. Advanced Functional Materials, 2016, 26, 3417-3423.	7.8	229
24	Photoexcitation dynamics in solution-processed formamidinium lead iodide perovskite thin films for solar cell applications. Light: Science and Applications, 2016, 5, e16056-e16056.	7.7	194
25	Phenylalkylamine Passivation of Organolead Halide Perovskites Enabling Highâ€Efficiency and Airâ€Stable Photovoltaic Cells. Advanced Materials, 2016, 28, 9986-9992.	11.1	532
26	Unusual thermal transport behavior in self-assembled fullerene nanorods. RSC Advances, 2016, 6, 67509-67513.	1.7	2
27	Distribution of bromine in mixed iodide–bromide organolead perovskites and its impact on photovoltaic performance. Journal of Materials Chemistry A, 2016, 4, 16191-16197.	5.2	29
28	Photoluminescence Enhancement in Formamidinium Lead Iodide Thin Films. Advanced Functional Materials, 2016, 26, 4653-4659.	7.8	61
29	Porous Pbl <sub>2</sub> films for the fabrication of efficient, stable perovskite solar cells via sequential deposition. Journal of Materials Chemistry A, 2016, 4, 10223-10230.	5.2	56
30	Carrier-Activated Polarization in Organometal Halide Perovskites. Journal of Physical Chemistry C, 2016, 120, 2536-2541.	1.5	27
31	A NIR-driven photocatalyst based on α-NaYF 4 :Yb,Tm@TiO 2 core–shell structure supported on reduced graphene oxide. Applied Catalysis B: Environmental, 2016, 182, 184-192.	10.8	126
32	HPbI <sub>3</sub> : A New Precursor Compound for Highly Efficient Solutionâ€Processed Perovskite Solar Cells. Advanced Functional Materials, 2015, 25, 1120-1126.	7.8	293
33	Composition-Dependent Light-Induced Dipole Moment Change in Organometal Halide Perovskites. Journal of Physical Chemistry C, 2015, 119, 1253-1259.	1.5	53
34	Pt <sub>3</sub> Co Concave Nanocubes: Synthesis, Formation Understanding, and Enhanced Catalytic Activity toward Hydrogenation of Styrene. Chemistry - A European Journal, 2014, 20, 1753-1759.	1.7	37
35	Fabrication of well-defined electromagnetic Fe <sub>3</sub> O <sub>4</sub> /polyaniline hollow microspheres and their application in Pb <sup>2+</sup> uptake. Polymer Chemistry, 2014, 5, 4332-4338.	1.9	11
36	Porous Pd nanoparticles with high photothermal conversion efficiency for efficient ablation of cancer cells. Nanoscale, 2014, 6, 4345-4351.	2.8	139

#	Article	IF	CITATIONS
37	The Role of Chlorine in the Formation Process of "CH <sub>3</sub> NH <sub>3</sub> Pbl <sub>3â€x</sub> Cl <sub>x</sub> ―Perovskite. Advanced Functional Materials, 2014, 24, 7102-7108.	7.8	294
38	Selective fluorescence response and magnetic separation probe for 2,4,6-trinitrotoluene based on iron oxide magnetic nanoparticles. Analytical and Bioanalytical Chemistry, 2013, 405, 4905-4912.	1.9	17
39	Anisotropic Overgrowth of Metal Heterostructures Induced by a Site‧elective Silica Coating. Angewandte Chemie - International Edition, 2013, 52, 10344-10348.	7.2	139
40	Metal Nanocrystalâ€Embedded Hollow Mesoporous TiO <sub>2</sub> and ZrO <sub>2</sub> Microspheres Prepared with Polystyrene Nanospheres as Carriers and Templates. Advanced Functional Materials, 2013, 23, 2137-2144.	7.8	112
41	Loading Metal Nanostructures on Cotton Fabrics as Recyclable Catalysts. Small, 2013, 9, 1003-1007.	5.2	29
42	Plasmonic Harvesting of Light Energy for Suzuki Coupling Reactions. Journal of the American Chemical Society, 2013, 135, 5588-5601.	6.6	597
43	Plasmon-enhanced chemical reactions. Journal of Materials Chemistry A, 2013, 1, 5790.	5.2	257
44	Ultrasound, pH, and Magnetically Responsive Crown-Ether-Coated Core/Shell Nanoparticles as Drug Encapsulation and Release Systems. ACS Applied Materials & Interfaces, 2013, 5, 1566-1574.	4.0	122
45	One-pot synthesis of In2S3 nanosheets/graphene composites with enhanced visible-light photocatalytic activity. Applied Catalysis B: Environmental, 2013, 129, 80-88.	10.8	145
46	Anisotropic Overgrowth of Metal Heterostructures Induced by a Siteâ€Selective Silica Coating. Angewandte Chemie, 2013, 125, 10534-10538.	1.6	21
47	Photocytotoxicity and Magnetic Relaxivity Responses of Dual-Porous γ-Fe <sub>2</sub> O <sub>3</sub> @ <i>meso</i> -SiO <sub>2</sub> Microspheres. ACS Applied Materials & Interfaces, 2012, 4, 2033-2040.	4.0	51
48	Plasmonic Percolation: Plasmon-Manifested Dielectric-to-Metal Transition. ACS Nano, 2012, 6, 7162-7171.	7.3	89
49	Porous Singleâ€Crystalline Palladium Nanoparticles with High Catalytic Activities. Angewandte Chemie - International Edition, 2012, 51, 4872-4876.	7.2	206
50	Selective Heteroepitaxial Nanocrystal Growth of Rare Earth Fluorides on Sodium Chloride: Synthesis and Density Functional Calculations. Angewandte Chemie - International Edition, 2012, 51, 8796-8799.	7.2	28
51	Red phosphorus: An elemental photocatalyst for hydrogen formation from water. Applied Catalysis B: Environmental, 2012, 111-112, 409-414.	10.8	265
52	Hierarchical P/YPO4 microsphere for photocatalytic hydrogen production from water under visible light irradiation. Applied Catalysis B: Environmental, 2012, 119-120, 267-272.	10.8	79
53	WO3/TiO2 microstructures for enhanced photocatalytic oxidation. Separation and Purification Technology, 2012, 91, 67-72.	3.9	26
54	Hexagonal tungsten trioxide nanorods as a rapid adsorbent for methylene blue. Separation and Purification Technology, 2012, 91, 103-107.	3.9	32

#	Article	IF	CITATIONS
55	Hierarchical core/shell Fe3O4@SiO2@γ-AlOOH@Au micro/nanoflowers for protein immobilization. Chemical Communications, 2011, 47, 2514.	2.2	56
56	Synthesis of Biocompatible, Mesoporous Fe <sub>3</sub> O <sub>4</sub> Nano/Microspheres with Large Surface Area for Magnetic Resonance Imaging and Therapeutic Applications. ACS Applied Materials & Interfaces, 2011, 3, 237-244.	4.0	197
57	Heteroepitaxial Growth of High-Index-Faceted Palladium Nanoshells and Their Catalytic Performance. Journal of the American Chemical Society, 2011, 133, 1106-1111.	6.6	287
58	Semiconductor/biomolecular composites for solar energy applications. Energy and Environmental Science, 2011, 4, 100-113.	15.6	75
59	Facile synthesis of size-controllable monodispersed ferrite nanospheres. Journal of Materials Chemistry, 2010, 20, 5086.	6.7	197
60	Induced Crystallization of Rubrene in Thinâ€Film Transistors. Advanced Materials, 2010, 22, 3242-3246.	11.1	67
61	NaYF4:Yb,Tm/CdS composite as a novel near-infrared-driven photocatalyst. Applied Catalysis B: Environmental, 2010, 100, 433-439.	10.8	165
62	Heteroepitaxial Growth of Core–Shell and Core–Multishell Nanocrystals Composed of Palladium and Gold. Small, 2010, 6, 2566-2575.	5.2	94
63	Green synthesis of a self-assembled rutile mesocrystalline photocatalyst. CrystEngComm, 2010, 12, 1759.	1.3	84
64	Growth of single-crystalline SnO <sub>2</sub> nanocubes via a hydrothermal route. CrystEngComm, 2010, 12, 341-343.	1.3	28
65	Growth of Tetrahexahedral Gold Nanocrystals with High-Index Facets. Journal of the American Chemical Society, 2009, 131, 16350-16351.	6.6	357
66	Copolypeptide-doped polyaniline nanofibers for electrochemical detection of ultratrace trinitrotoluene. Talanta, 2009, 79, 376-382.	2.9	56
67	Amine-Capped ZnSâ~'Mn <sup>2+</sup> Nanocrystals for Fluorescence Detection of Trace TNT Explosive. Analytical Chemistry, 2008, 80, 3458-3465.	3.2	346
68	Strongly Coupled Excitonic States in H-Aggregated Single Crystalline Nanoparticles of 2,5-Bis(4-methoxybenzylidene) Cyclopentanone. Journal of Physical Chemistry B, 2008, 112, 2837-2841.	1.2	25
69	General Properties of Local Plasmons in Metal Nanostructures. Physical Review Letters, 2006, 97, 206806.	2.9	446